Nuclear Instruments and Methods in Physics Research B 371 (2016) 273–277

Contents lists available at ScienceDirect

Nuclear Instruments and Methods in Physics Research B

journal homepage: www.elsevier.com/locate/nimb

Effect of water on solid electrolyte interphase formation in Li-ion batteries

M. Saito [a,*], M. Fujita [a], Y. Aoki [a], M. Yoshikawa [a], K. Yasuda [b], R. Ishigami [c], Y. Nakata [c]

[a] Toray Research Center Inc., 3-3-7, Sonoyama, Otsu, Shiga 520-0842, Japan
[b] Kyoto Prefectural University, 1-5, Hangi-cho, Shimogamo, Sakyo-ku, Kyoto, Kyoto 606-8522, Japan
[c] The Wakasa Wan Energy Research Center, 64-52-1, Nagatani, Tsuruga, Fukui 914-0192, Japan

ARTICLE INFO

Article history:
Received 1 July 2015
Received in revised form 9 September 2015
Accepted 9 September 2015
Available online 29 September 2015

Keywords:
TOF-ERDA
XPS
GC/IC
^{1}H NMR
Lithium ion battery

ABSTRACT

Time-of-flight-elastic recoil detection analysis (TOF-ERDA) with 20 MeV Cu ions has been applied to measure the depth profiles of solid electrolyte interphase (SEI) layers on the negative electrode of lithium ion batteries (LIB). In order to obtain quantitative depth profiles, the detector efficiency was first assessed, and the test highlighted a strong mass and energy dependence of the recoiled particles, especially H and He. Subsequently, we prepared LIB cells with different water contents in the electrolyte, and subjected them to different charge–discharge cycle tests. TOF-ERDA, X-ray photoelectron spectrometry (XPS), gas chromatography (GC), ion chromatography (IC), and ^{1}H nuclear magnetic resonance (^{1}H NMR) were applied to characterize the SEI region of the negative electrode. The results showed that the SEI layer is formed after 300 cycle tests, and a 500 ppm water concentration in the electrolyte does not appear to cause significant differences in the elemental and organic content of the SEI.

1. Introduction

Over the past several years, significant progress has been made in the technology of electrodes and electrolytes used in lithium ion batteries (LIBs). However, the reduced battery lifetime due to capacity fading during charging and discharging still represents a major problem [1]. One of the possible reasons for the fading phenomenon could be the formation of a solid electrolyte interphase (SEI) layer on the electrode surfaces [2], by electrolyte degradation or by migration of lithium. On the other hand, the SEI could also work as a kind of passivation layer, and stop further decomposition of the organic electrolyte. As a result, depending on its characteristic, the SEI may preserve the integrity of the electrodes, allowing them to retain their high reversible capacity and good cycling ability [3,4]. These considerations have fuelled extensive research, aimed to understand the process and mechanism of SEI formation using various experimental techniques, such X-ray photoelectron spectrometry (XPS) and time-of-flight secondary ion mass spectrometry (TOF-SIMS) [5,6]. Analytical techniques using energetic ion beams are powerful tools for determining quantitative depth profiles with good accuracy. Among these methods, time-of-flight elastic recoil detection analysis (TOF-ERDA) is particularly suitable for the measurement of light elements, including H and Li, with a depth resolution down to 4 nm [7–10]. In this work, we applied TOF-ERDA analysis for the quantitative measurement of the depth profiles of the SEI layer. For this purpose, we first assessed the efficiency of the detector in our TOF-ERDA setup, and then we studied the effect of the water content in the electrolyte on the SEI formation by means of TOF-ERDA, XPS, gas and ion chromatography (GC and IC, respectively), and ^{1}H NMR analysis.

2. Experiments

2.1. Sample preparation

A laminate (stacked)-type cell with $LiNiCoMnO_2$ and graphite as positive and negative electrodes, respectively, was used for the preparation of the LIB sample. The electrolyte consisted of 1 M $LiPF_6$ dissolved in 1:1 ethylene carbonate/diethylcarbonate. In order to evaluate the effect of the water content in the electrolyte on the formation of the SEI, we prepared two different electrolyte samples, with and without water: the first (hereafter labeled “500 ppm” sample) contained 500 ppm of H_2O, and the second (labeled “dewatered”) was dewatered to a H_2O content below 30 ppm. Subsequently, a charge–discharge cycle test was conducted, in which the cells were charged with constant current

---

* Corresponding author at: Toray Research Center Inc., Surface Science Laboratory, 3-3-7, Sonoyama, Otsu, Shiga 520-0842, Japan. Tel.: +81 77 533 8657; fax: +81 77 533 8607.

E-mail address: Masahiro_Saito@trc.toray.co.jp (M. Saito).

http://dx.doi.org/10.1016/j.nimb.2015.09.033

(CC) at 1*C* rate (which means that the discharge current will fully discharge the battery in 1 h), to reach 4.3 V, and then discharged to 3.0 V, again at 1*C* rate. Two different charge/discharge cycling conditions were used for each sample: the first involved one single cycle, and the second 300 cycles, giving a total of four samples to be analyzed, combining two different water contents with two different cycling conditions. The LIB cells were then disassembled in an argon-filled glove box, whose dew point was below −84 °C, and the negative electrodes were collected and introduced into a target chamber under N_2 atmosphere (dew point of approximately −50 °C), in such a way to avoid air exposure.

2.2. Sample characterization

Since the details of the TOF-ERDA experimental setup used in this work were presented in a previous report [10], only a brief description and some differences are highlighted here. The TOF-ERDA system consists of two time detectors and a silicon surface-barrier detector (SSD). The detection angle is 40° with respect to the beam direction. The time detector, positioned in the flight path, includes a micro channel plate (MCP) detector, an electrostatic mirror grid [11], and a carbon foil with a thickness of 3 $\mu g/cm^2$ (on the sample side) and 10 $\mu g/cm^2$ (on the SSD side). The length of the flight path, corresponding to the distance between the front and the rear of the carbon foil, is 611 mm, and the solid angle of this system is 3×10^{-4} sr. The time resolution of the TOF measurement system is 0.39 ns. Since the so-called pulse height defect [12,13] makes the accurate calibration of the energy of different ion species measured by SSD problematic, the energies of the recoiled particles were measured by TOF. The TOF measurements have a better energy resolution for heavier elements than SSD [14] and the calibration does not depend on a specific mass.

The efficiency of the time detector was assessed using $^{1}H^{+}$, $^{4}He^{+}$, and $^{12}C^{+}$ beams, whose energies are shown in Table 1. The ions scattered from a 200 μm-thick Au target bombarded with these ions were detected by TOF and SSD. TOF-ERDA measurements were carried out using 20.0 MeV $^{63}Cu^{12+}$ beams, with a dosage of approximately 0.7 μC per sample. The incident and exit angle were 30° and 10°, respectively, where the incident (exit) angle is defined as the angle between incident beam and surface normal. XPS analysis was carried out using a monochromatic Al Kα line ($h\nu$ = 486.6 eV), and the photoelectron take-off angle was 45°. Gas and ion chromatography analyses were performed using a thermal conductivity and an electrical conductivity detector, respectively. The samples for the ^{1}H NMR analysis were extracted with D_2O solvent and then calibrated using 2,2,3,3-d4-3-(trimethyl silyl)propionic acid sodium salt (TSP) as internal standard.

3. Results and discussion

3.1. Evaluation of detector efficiency

Since TOF spectrometers based on a carbon foil time pick-up detector have some known issues with the detection efficiency, which is energy- and ion-dependent and usually lower than 100% for light elements [15,16], we evaluated the detection efficiency for the present setup initially. Assuming that all particles are detected with the SSD, we can define the detector efficiency η as the ratio of particles detected in coincidence (SSD and TOF) to those detected without coincidence (SSD only). The detector efficiency estimated in this way is plotted in Fig. 1 as a function of the energy. The detection efficiency for carbon is stable in a wide energy range; however, as for H and He, the efficiency shows a strong dependence on the energy. According to reference [15], the detector efficiency of this kind of TOF systems is mainly determined by the statistics of secondary electron production from a foil free from holes, and is thus correlated with *dE/dx* in the foil. Fig. 2 shows the dependence of η on the electronic stopping power, as well as the curve fitted using a sigmoid function. The fitted curve provides the η value for the elements of interest. In particular, the detection efficiency for Li, which is difficult to be used at our beamline, can be quantified by extrapolation from the same fitted curve. Another aspect worth mentioning is that although the detection efficiency of carbon is stable, its saturated value is around 80%, whereas it was usually 100% in the previous report [15]. Whereas the reason for this discrepancy is still unclear, a possible explanation is that a fraction of the secondary electrons generated by the carbon foil may escape detection by the MCP detector.

Table 1
Incident ions and corresponding energy used in the evaluation of efficiency of the time detector.

Incident ion	Energy (MeV)
$^{1}H^{+}$	2.0
$^{4}He^{+}$	2.0, 5.7
$^{63}Cu^{12+}$	2.0, 10.0

3.2. TOF-ERDA analysis of the SEI layer

Fig. 3 shows the TOF versus energy plot (panel a) and the energy spectrum (panel b) of the dewatered sample after 300 cycles. The TOF curves of H, Li, C, O, and F are plotted in Fig. 3(a), whereas Fig. 3(b) only shows the oxygen energy spectrum as an example. The depth profile for each element was obtained from the energy spectrum, by applying the corresponding scattering cross-section, stopping power, and detector efficiency. No special software was used for this calculation. Fig. 4 shows the TOF-ERDA depth profile of the dewatered sample after one and 300 cycles (panels a and b, respectively). No surface layer is observed in Fig. 4(a), except for carbon. On the other hand, Fig. 4(b) highlights an increased Li, H, and O content in the surface region, which reflects the SEI formation after 300 cycles. Fig. 5 shows the depth profile of the 500 ppm sample, after one cycle (panel a) and 300 cycles (panel b). The same trend as in Fig. 4 was found, with the SEI layer formation observed only after 300 cycles. After comparing the SEI layers from both samples, we concluded that no significant differences were present in the SEI region between the two samples. The com-

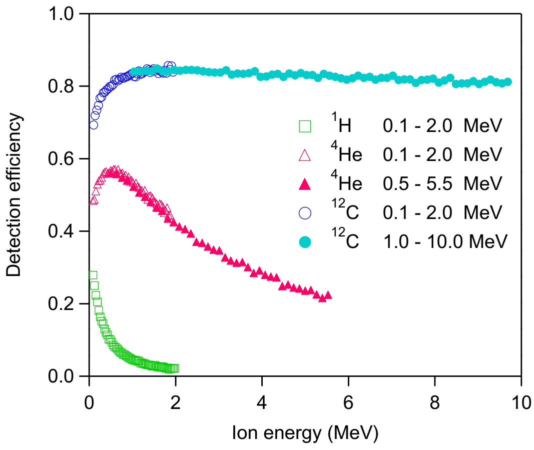

Fig. 1. Detector efficiency η for hydrogen, helium, and carbon as a function of energy.